Process Integration of Heat Pump Storage Systems Using Time-Resolved Data

Jasper V. M. Walden[a,*], Roger Padullés[a], Daniel Nørhave[a,b], Wiebke Meesenburg[a], A. Phong Tran[c]

[a]Department of Civil and Mechanical Engineering, Technical University of Denmark, 2800 Kgs. Lyngby, Denmark
[b]Danish Technological Institute, Energy and Climate, Taastrup 2630, Denmark
[c]German Aerospace Center (DLR), Institute of Low-Carbon Industrial Processes, 03046 Cottbus, Germany
*Corresponding author: jvmwa@dtu.dk

Abstract

This study explores the use of time-resolved process data to support the design of flexible and efficient industrial heat pump systems. Building concepts from dynamic process integration, such as Dynamic Pinch Analysis, the work proposes a method to quantify the flexibility requirements for heat pump operation under varying process conditions. In addition to informing operational strategies, the time-resolved data are shown to be valuable for the design of heat pump storage systems. A typical configuration includes thermal storage tanks on both the source and sink sides, allowing the system to buffer fluctuations in heat availability and demand. By stabilizing the source temperature, storage improves heat pump efficiency, increases heat coverage, and raises the degree of electrification. The presented approach outlines how time-resolved data and mathematical optimization can guide the sizing and integration of such systems to enhance both energy and economic performance in industrial electrification strategies. The methodology was applied to an automotive paint shop process showing large potential by reducing operational expenditures by 27.4 %.

Keywords: Industrial Heat Pump, Heat Pump Storage System, Flexibility, Electrification of Industry

1. Introduction

Electrification of sectors such as buildings, transport and industry has been outlined as major pathway to decarbonization [1,2]. Within industry, most energy is consumed to generate process heat. Particularly, process heat below 300 °C can be electrified highly efficiently by industrial heat pumps [3,4] employing direct electrification [5]. However, in the EU currently only 3 % of industrial process heat is electrified [6]. Barriers to industrial electrification mainly come from four pillars: economic, technological, infrastructural and knowledge-based concerns [7]. While OPEX parity can be reached in some countries due to favorable electricity-to-fuel/gas price ratios [8], concerns include the ability of industrial heat pumps to supply fluctuating process demands.

Of course, present Process Integration literature has already addressed heat pump storage integration. Schlosser et al. [9] investigated the integration of a heat pump storage system (HPS) into a manufacturing process by using the time-average model and source-sink profiles to size the HPS and the heat recovery loop (HRL). The study found that 83 % of heating and 48 % of cooling demands can be covered by the HPS. To avoid expensive mathematical formulations, Stampfli et al. [10] investigated the integration of a HPS by applying an insight-based hybrid method to restrict the solution space of the mathematical optimization problem. The method was applied to a dairy site and has shown that the introduced hybrid method achieves realistic approach temperatures in the condenser and evaporator of the heat pump in contrast to the insight-based method. The Indirect Source Sink Profiles (ISSP) are an engineer-centered method to practically integrate thermal energy storage (TES) into industrial processes. Agner et al. [11] extended the ISSP methodology to heat pump integration to result in a heat exchanger storage network (HESN) design. Agner et al. [12] also investigated the control challenges in such a system and proposed a two-layer control strategy, which tested with a dynamic simulation model. Furthermore, a variety of studies exist that employed HPS combined with operational optimization to leverage dynamic electricity tariffs and reduce the overall cost of heat supply [13–16]. Furthermore, a variety of studies on the process integration of TES [17,18] and studies on the flexibility of heat pumps [19–23] exist.

Previous studies often lack operational optimization, fail to account for the part-load capability of the heat pump, or neglect the optimization of the TES and HRL temperatures. Consequently, the present work introduces a two-stage, insight-based optimization model that determines the design parameters of the heat pump system (HPS) and optimizes its operation. The model explicitly considers the heat pump's part-load behavior in response to varying process heat demands across different temperature levels.

The approach consists of two stages:

1. At the design stage: optimization of the four source- and sink-side temperatures of the HPS HRL, the capacities of both TES units, and the nominal heating capacity of the heat pump.
2. At the operational stage: optimization of the heat pump load, as well as the charge and discharge profiles of the sink- and source-side TES units at each timestep.

The next chapter introduces the methodology, including system design, problem formulation, and constraints to guarantee technical feasibility across all operating points.

2. Approach

The heat pump storage system suggested in this work is shown in Figure 1 and is very similar to the HPS presented in [9,10,12]. At its core a heat pump drives cold and hot utility system. To buffer fluctuations to and from the process at both, heat pump source and sink side, a heat storage is installed. The heat pumps heat exchangers inlet/outlet temperatures match the storage temperatures. Any additional heating or cooling requirements higher or lower than that of the intermediate heat pump storage loop can be achieved by additional hot or cold utility ($\dot{Q}_{\mathrm{HU}}/\dot{Q}_{\mathrm{CU}}$). The required process heating or cooling demand is given by a temperature heat load profile indicating the heating demand at each temperature and vice-versa for process cooling.

The design variables at the system levels are, consequently: heat sink inlet/outlet temperature, heat source inlet/outlet temperature, mass of the storages and the heating capacity of the heat pump.

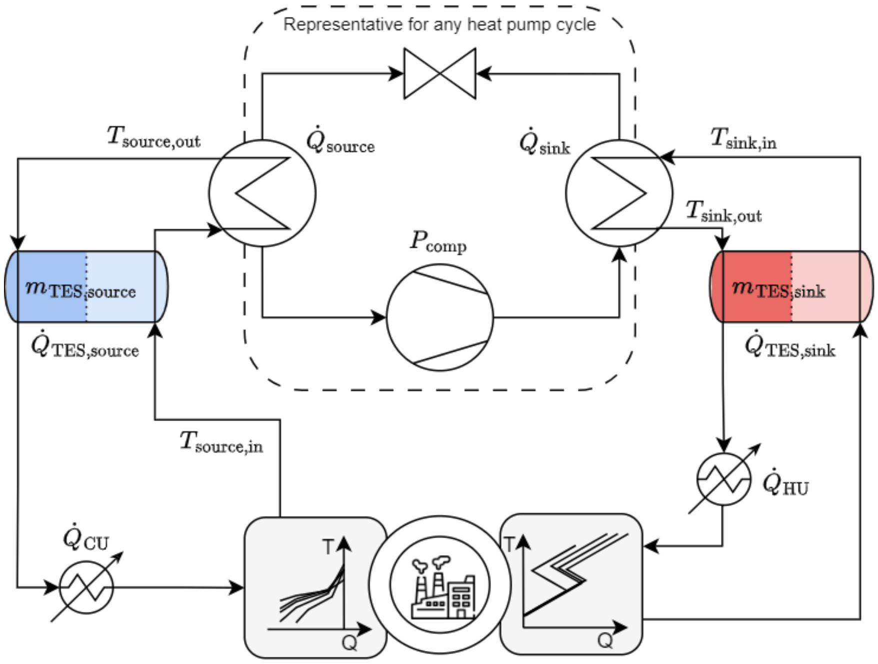

Figure 1: Investigated heat pump storage system configuration.

2.1. Optimization approach

Analogous, the optimization is set up. The system is thought to provide additional flexibility and due to the process fluctuating, a new operating condition is set at every time step. Thus, after selecting design variables, the operation of the system needs to be solved for minimal operating expenditures (OPEX). This has an influence on the choice of design variables as there is a trade-off between capital expenditures (CAPEX) and OPEX. Due to this, the optimization problem was set up two be solved in two-stages: (1) the design stage and (2) the operational optimization. The design stage maximizes net present value (NPV).

A flowchart of how the optimization progresses is shown in Figure 2. The input parameters are shown in Table 1 & 2. The design optimization runs a few pre-calculations based on the design parameters, such as a temperature feasibility check, pinch temperature violations and calculates the maximum heat that can be delivered by the heat pump storage system at each timestep while still maintaining heat transfer. These are the constraints within the design optimization carried out through SciPy's differential evolution [24]. This then passes the Q_{max} and design vector p to the operational optimization, which is carried out by Pyomo [25,26] minimizing OPEX and determining the used heat loads of the TES and HP respective to its part load efficiency [22].

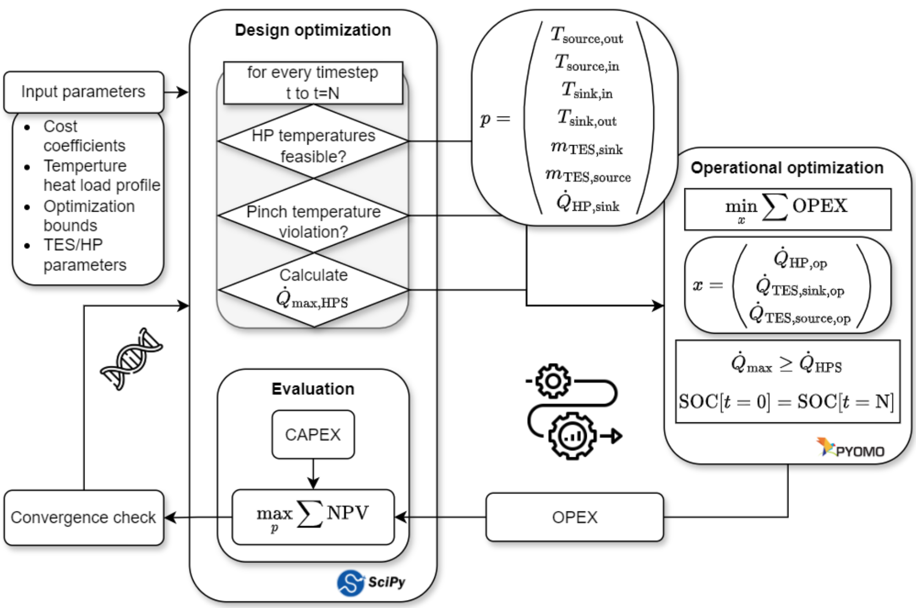

Figure 2: Flowchart of the optimization decomposition strategy.

The design optimization problem can be written as:

$$\max_{p} \; NPV \tag{1}$$

$$p = [T_{source,in}, T_{source,out}, T_{sink,out}, T_{sink,in}, \dot{Q}_{HP}, m_{TES,sink}, m_{TES,source}] \tag{2}$$

subject to:

$$T_{source,in} \geq T_{source,out} \tag{3}$$

$$T_{sink,out} \geq T_{sink,in} \tag{4}$$

$$T_{sink,in} > T_{source,in} \tag{5}$$

$$T_{sink,in} > PT^{t} + \Delta T_{min,hp} \tag{6}$$

$$PT^{t} + \Delta T_{min,hp} > T_{source,in} \tag{7}$$

The maximum heat load that can be provided by the HPS without temperature crossover ($\dot{Q}_{\mathrm{max,HPS,sink/source}}$) is determined by the intersection between sink (or source) temperature-heat load profile and the HPS system (see Eq. 10). For simpler notation, the usually piecewise-linear temperature-heat load profile is written as $g_{demand}(x)$

$$f_{HPS}(z) = \frac{T_{sink,out} - T_{sink,in}}{\dot{Q}_{HP} + \dot{Q}_{TES}} z + T_{sink,in} \tag{8}$$

$$h(z) = f_{HPS}(z) - g_{demand}(z) \tag{9}$$

$$h(\dot{Q}_{max,HPS,sink/source}) = 0 \tag{10}$$

The operational optimization problem is:

$$\min_{x} \; OPEX \tag{11}$$

$$p = [\dot{Q}_{HP,op}, \dot{Q}_{TES,sink,op}, \dot{Q}_{TES,source,op}] \tag{12}$$

Subject to:

$$\dot{Q}_{max,HPS} \geq \dot{Q}_{HPS,op} \tag{13}$$

$$SOC_{TES}[t = 0] = SOC_{TES}[t = N] \tag{14}$$

Where Eq. 13 applies to both sink and source side.

2.2. Modelling

The heat pump modelling was based on a Lorenz efficiency approach in which $\bar{T}$ logarithmic mean temperature difference. To model the efficiency change in part load the polynomial developed in [22] was used.

$$COP_{design} = \eta_{Lor} \frac{\bar{T}_{sink}}{\bar{T}_{sink} - \bar{T}_{source}} \tag{16}$$

$$COP_{op}^{t} = \eta_{PL} \cdot COP_{design} \text{ with } \eta_{PL} = f\left(\frac{\dot{Q}_{HP,op}^{t}}{\dot{Q}_{HP}}\right) \tag{17}$$

$$W_{HP}^{t} = \frac{\dot{Q}_{HP,op}^{t}}{COP} \tag{18}$$

The TES was assumed to be a fixed volume stratified tank. Consequently, there is no heat transfer but rather mass going in and out of the tank. For now, no heat loss of the tank was considered in modelling. The heat flow $(\dot{Q}_{TES,op})$ was considered positive, when the TES is discharging and negative when charging. This convention was chosen as it is adding or removing heat to the heat pump HRL. Thus, the TES modelling was an simple energy balance and the state of charge of the TES is determined by Eq. 19.

$$SOC[t] = SOC[t-1] - \dot{Q}_{TES,op} \tag{19}$$

The energy balance determined the remaining process requirements by hot and cold utilities, as per Eq. 20-21.

$$\dot{Q}_{HU}^{t} = \dot{Q}_{h,demand}^{t} - \left(\dot{Q}_{HP,op}^{t} + \dot{Q}_{TES,sink,op}\right) \tag{20}$$

$$\dot{Q}_{CU}^{t} = \dot{Q}_{c,demand}^{t} - \left(\dot{Q}_{HP,source,op}^{t} + \dot{Q}_{TES,source,op}\right) \tag{21}$$

The CAPEX of the TES' and heat pump were calculated using Eq. 22 & 23.

$$CAPEX_{TES} = \alpha_{TES} \cdot V_{TES}^{-0.47} \tag{22}$$

$$CAPEX_{HP} = \alpha_{HP} \cdot \dot{Q}_{HP} \tag{23}$$

The OPEX were determined by summing up the OPEX of each timestep.

$$OPEX_{HP} = \sum_{t=0}^{N} W_{HP,op}^{t} \cdot p_{elec} \tag{24}$$

$$OPEX_{HU} = \sum_{t=0}^{N} \dot{Q}_{HU}^{t} \cdot p_{HU} \tag{25}$$

$$OPEX_{CU} = \sum_{t=0}^{N} \dot{Q}_{CU}^{t} \cdot p_{CU} \tag{26}$$

2.3. Parameters

The above equations are used along with the economic parameters presented in Table 1.

Table 1. Economic parameters.

	p_{elec} (€/MWh)	p_{HU} (€/MWh)	p_{CU} (€/MWh)	α_{HP} (€/kW)	α_{TES} (€/m³)	Discount rate (%)	Fin. Lifetime (y)
Value	113	72	38	500	7450	7	20
Reference	[27]	[28]	[27]	[23]	[29]	[30]	-

Furthermore, the efficiency and TES parameters are shown in Table 2. The TES fluid is assumed to be water.

Table 2. Heat pump and TES parameters.

	η_{Lor} %	$c_{p_{TES}}$ (kJ/kgK)	ρ_{fluid} (kg/m³)
Value	60	4.184	997
Reference	[31]	[32]	[32]

2.4 Case Study

The method was applied to the simulation of a top-coat line of an automotive paint shop. The line includes a base coat spray booth, a flash-off dryer, a clear coat spray booth, and a final drying oven. In the base coat booth, the visible color layer is applied, followed by a flash-off stage operating at 60–80 °C to allow controlled drying of the water-based paint without boiling. The clear coat is then applied in a second spray booth and cured in a high-temperature drying oven operated between 140–180 °C.

Spray booths require tightly controlled air temperature and humidity and have large air volume flow rates which leads to high HVAC energy demand. The drying ovens similarly operate with large airflows and elevated temperatures, contributing to the overall thermal energy consumption. The production schedule

follows a continuous three-shift operation from Monday to Friday, with each shift lasting eight hours and including short breaks for shift changes and lunch. HVAC and heating systems are started two hours before the first shift to ensure adequate flushing and temperature stabilization before coating operations begin. The paint shop was modelled in Modelica and simulated for an entire year with a timestep of an hour.
In this work, the Grand Composite Curve is used with a $\Delta T_{\min}$ of 20 K. The GCC already shifts the temperatures by ½ $\Delta T_{\min}$, consequently that is considered the approach temperature for the HP-TES-HRL.

3. Results & Discussion

After running the optimization for the entire year, the results of the optimization variables are analyzed below. Firstly, the design variables (Eq. 2) are presented in Table 3.

Table 3. Resulting design variables.

	$T_{\text{source,in}}$ (°C)	$T_{\text{source,out}}$ (°C)	$T_{\text{sink,out}}$ (°C)	$T_{\text{sink,in}}$ (°C)	$\dot{Q}_{\text{HP}}$ (kW)	$m_{\text{TES,sink}}$ (t)	$m_{\text{TES,source}}$ (t)	$\text{COP}_{\text{mean/max}}$ (-)
HP	-10.1	-13.6	108.4	34	1993	0.0	0.0	2.1/2.5
HP+TES	-6.7	-6.8	43.6	36.5	1921	10.1	2.4	3.2/4.0

The operational optimization and the selection of decision variables across all 8 760 timesteps are illustrated in Figure 3. The upper part of the figure shows the source side, while the lower part represents the sink side. The overall cooling demand (dark blue) follows a seasonal pattern with lower cooling requirements in winter, whereas the heating demand is slightly reduced in summer.

The zoomed section of Figure 3 shows the operating variables for a two-week period. At the beginning of the first week, a start-up peak in heat demand occurs. During this week, several fluctuations can be observed. For instance, at hour 6250, the heating demand drops while the cooling demand increases, which reduces the cooling supplied by the HPS and raises the demand for cold utility. As a result, the heat pump operates in part load during this period. The purple line indicates the maximum deliverable heat of the HPS ($\dot{Q}_{\text{max,HPS,sink}}$), constrained by feasible heat transfer. Around timestep 6300, the HPS reaches this limit, and the remaining heat demand must be covered by hot utility.
In contrast, the second zoomed week exhibits more stable heating and cooling demands. Here, the heat pump operates continuously at design load, and any residual fluctuations are balanced by hot and cold utility. On the sink side, the TES shows buffering capabilities, alternating between charging and discharging with loads of around 200 kW over the analysed two-week period. On the source side, TES heat loads of approximately 20 kW are almost negligible in this interval.

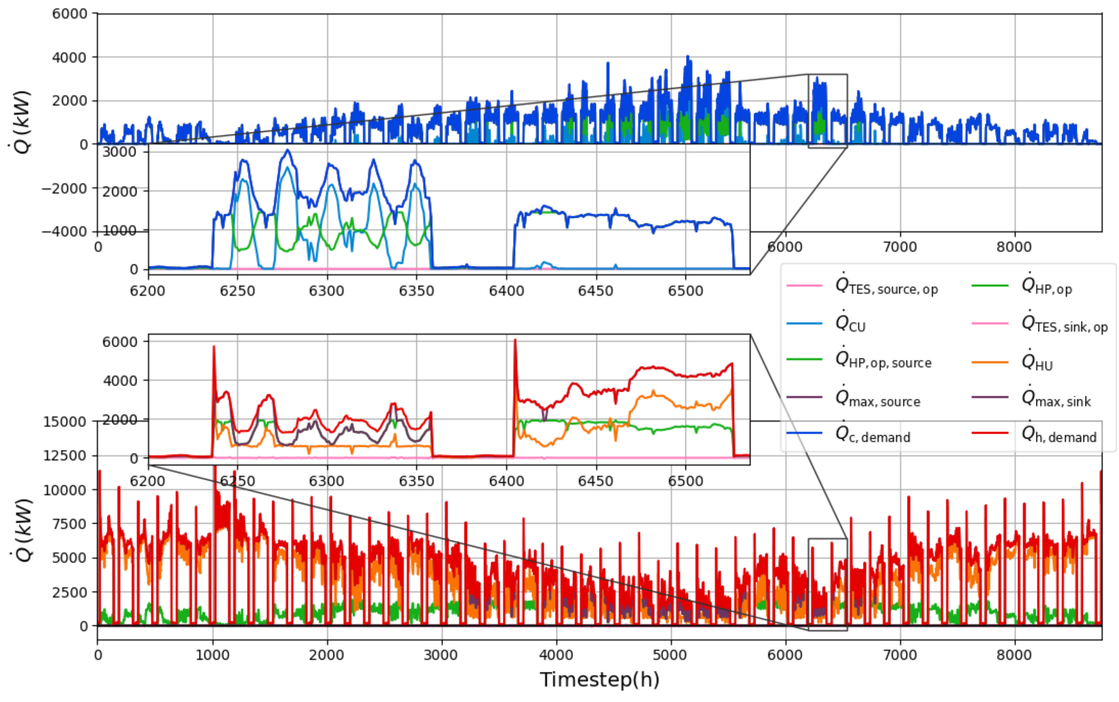

Figure 3: Annual time series of operating variables for the heat pump system, including process heating and cooling demands, utility use, and thermal energy storage operation.

Figure 4 depicts a load duration curve of both sink- (left) and source (right) sides. At ~ 4700 hours, $\dot{Q}_{\mathrm{max,HPS,sink}}$ becomes lower than the heating demand ($\dot{Q}_{\mathrm{h,demand}}$), which means for about 1500 hours the HPS can deliver less heat due to the temperature heat transfer constraint (Eq. 8-10). In other words, the process requires less heat at the temperature of the HRL than what the HRL could provide. Besides, the HP operates about 2000 hours at base load. From the right side of the Figure, it becomes apparent that the heat pump operation is mainly constrained by the available source heat or source cooling demand. Particularly when there is not enough source heat available, the HPS is forced into part load operation.
Over the analysed year, the HPS supplies 28.5 % of the total process heating requirement and 74.5 % of total process cooling requirement. This sums to 7393 MWh of heating; 1943 MWh of electricity and 5449 MWh of cooling.

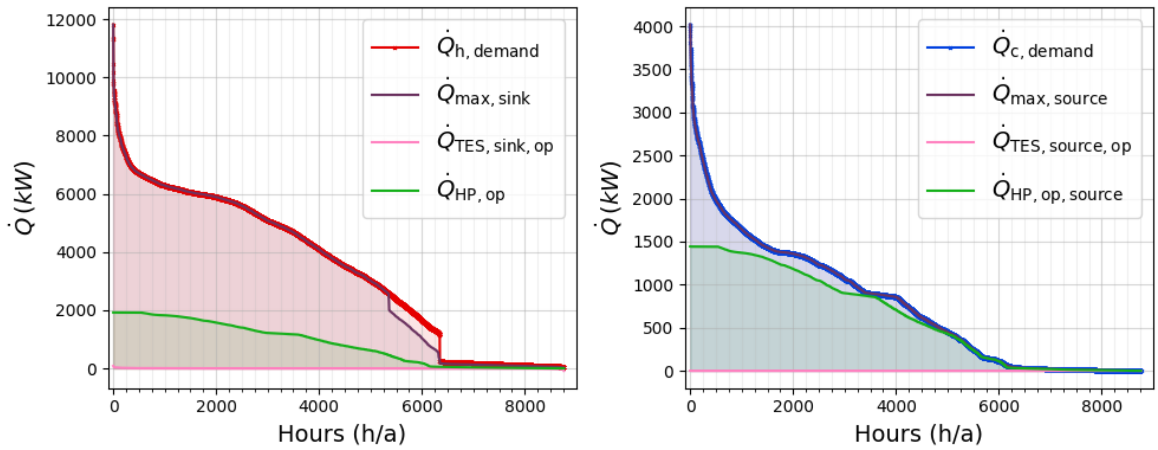

Figure 4: Load duration curves of heat- and cooling demand and supply.

Besides the dependencies prescribed by the model equations, examining the correlations between the resulting variables provides additional insight. Top left in Figure 5, a correlation between overall heating and cooling demand is shown. As previously discussed, cooling demand increases at higher ambient temperatures, while the corresponding heating demand decreases.

The bottom-left plot illustrates the strong correlation between cooling demand and heat pump operation. As cooling demand rises, the heat pump load increases until it reaches its design capacity; any further increase in cooling demand must then be met by additional cold utility. For even higher cooling demands, the heat pump load decreases again because the associated reduction in heating demand pushes the heat pump back into part-load operation.

The right-hand side of Figure 5 illustrates the behaviour of the TES in relation to heat pump load. The top-right plot links the source-side TES to the heat pump heat-source load and shows no clear correlation, reflecting the generally small source TES heat flows and its primarily buffering role. The sink-side TES, in contrast, exhibits higher charging and discharging rates as the heat pump is operated at higher loads, which is consistent with larger surplus or deficit heat quantities at the sink.

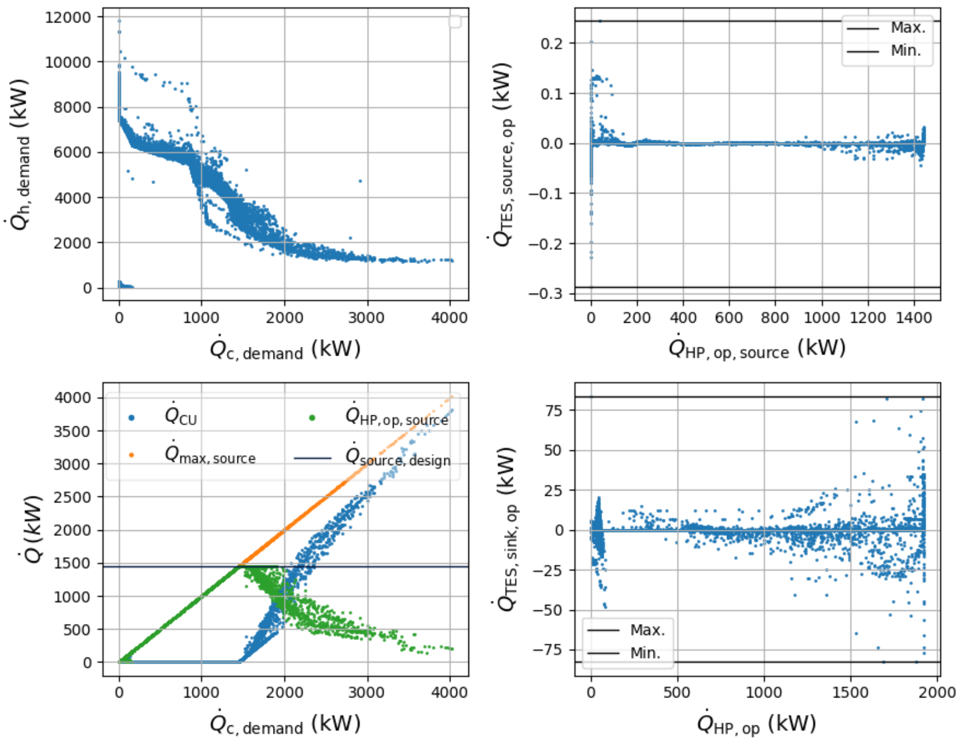

Figure 5: Correlations between operating parameters.

Regarding the choice of heat pump and heat pump cycle, the determined temperature levels point to a two-stage configuration with R601 as refrigerant, as identified from the simulation database of Andersen et al. [33].

The maximum charge and discharge heat loads of the sink-side TES are 84 kW and 83 kW, whereas the corresponding values for the source-side TES are 0 kW. To quantify utilization, the sink-side TES cycles 21 MWh of thermal energy over the year, while the source-side TES cycles only 26 kWh. This shows that the sink TES is actively used as an operational buffer, whereas the source TES provides very limited smoothing of the heat source.

Finally, Table 4 breaks down the resulting economic parameters. The key point is the absolute savings in OPEX when using the suggested HPS, these add up to roughly 1,896 k€ annually. At CAPEX of 997,7 k€; this corresponds to a simple payback period of approximately 1.9 years, indicating a highly attractive investment. This displays in the high 20-year NPV of 4.5 M€.

Table 4. Economic evaluation.

	NPV	PBP	OPEX	Abs. OPEX savings	Rel. OPEX savings	Rel. CO2 savings	CAPEX TES_{sink}	CAPEX TES_{source}	CAPEX HP
	(k€)	(y)	(k€)	(k€)	(%)	(%)	(k€)	(k€)	(k€)
No Action	-	-	2,416	-	-	-	-	-	-
HP+TES	4,508	1.9	1,896	519.7	27.4	14	25,5	12	960,3

4. Conclusions

This work shows that time-resolved process data are a powerful basis for designing and operating flexible industrial heat pump storage systems. The proposed approach exploits Dynamic Pinch Analysis and mathematical optimization to determine how the heat pump should be dispatched and how source- and sink-side storage should be used under realistic, time-varying conditions. The approach also determines the optimal design temperatures for the HPS, while sizing heat pump and storages.

Over the analysed year, the proposed HPS supplies 28.5 % of the total process heating and 74.5 % of the total process cooling, corresponding to 7,393 MWh of heating delivered from 1,944 MWh of electricity and 5,449 MWh of cooling. The sink-side TES reaches charge/discharge powers of 84 kW and 83 kW and cycles 21 MWh annually, while the source-side TES is limited to 26 kWh, indicating that storage on the sink side acts as an actively used operational buffer, whereas the source-side storage provides modest smoothing of heat availability.

Economically, the integrated HPS–TES configuration achieves annual OPEX savings of roughly 1,896 k€ for a CAPEX of 998 k€, resulting in a simple payback time of roughly three years and a 20-year NPV of 4.5 M€, making the solution highly attractive under the given boundary conditions.

A key limitation of the current work is that ambient air (or other environmental sources) was not considered as an additional heat source, which could further improve heat coverage by the heat pump and its efficiency.

The inspiration for future work is manifold. The trade-off between heat pump temperature lift and required storage capacity should be examined in more detail. Furthermore, quantifying the benefits of allowing the HRL temperatures to vary dynamically during operation would provide deeper insight into flexibility and efficiency potential. Finally, to draw broader conclusions on industrial HPS design, the proposed methodology will be applied to a wider range of processes and boundary conditions.

Acknowledgements

This research project was funded by The Energy Technology Development and Demonstration Programme (EUDP), under the project 64020-1074 titled: "SuPrHeat – sustainable process heating with high-temperature heat pumps using NatRefs".

References

[1] United Nations, Seizing the moment of opportunity: Supercharging the new energy era of renewables, efficiency, and electrification, (2025). https://www.un.org/en/climatechange/moment-opportunity-2025.

[2] International Energy Agency, World Energy Outlook 2025, Paris, 2025. https://www.iea.org/reports/world-energy-outlook-2025.

[3] M. Rehfeldt, T. Fleiter, and F. Toro, A bottom-up estimation of the heating and cooling demand in European industry, *Energy Effic*. **11** (2018) 1057–1082. doi:10.1007/s12053-017-9571-y.

[4] W.B. Markussen, J. Rosenow, M.H. Christensen, B. Zühlsdorf, and B. Elmegaard, Techno-economic analysis of technologies for decarbonizing low- and medium-temperature industrial heat, *Cell Reports Sustainability*. (2025) 100560. doi:10.1016/j.crsus.2025.100560.

[5] O. Ruhnau, S. Bannik, S. Otten, A. Praktiknjo, and M. Robinius, Direct or indirect electrification? A review of heat generation and road transport decarbonisation scenarios for Germany 2050, *Energy*. **166** (2019) 989–999. doi:10.1016/j.energy.2018.10.114.

[6] R. de Boer, A. Marina, B. Zühlsdorf, C. Arpagaus, M. Bantle, V. Wilk, B. Elmegaard, J. Corberán, and J. Benson, Strengthening industrial heat pump innovation: Decarbonizing industrial heat, (2020).

[7] J. Rosenow, C. Arpagaus, S. Lechtenböhmer, S. Oxenaar, and E. Pusceddu, The heat is on: Policy solutions for industrial electrification, *Energy Res Soc Sci*. **127** (2025) 104227. doi:10.1016/j.erss.2025.104227.

[8] J.V.M. Walden, and R. Padullés, An analytical solution to optimal heat pump integration, *Energy Convers Manag*. **320** (2024) 118983. doi:10.1016/j.enconman.2024.118983.

[9] F. Schlosser, J.-P. Seevers, R.-H. Peesel, and T.G. Walmsley, System efficient integration of standby control and heat pump storage systems in manufacturing processes, *Energy*. **181** (2019) 395–406. doi:10.1016/j.energy.2019.05.113.

[10] J.A. Stampfli, M.J. Atkins, D.G. Olsen, M.R.W. Walmsley, and B. Wellig, Practical heat pump and storage integration into non-continuous processes: A hybrid approach utilizing insight based and nonlinear programming techniques, *Energy*. **182** (2019) 236–253. doi:10.1016/j.energy.2019.05.218.

[11] R. Agner, B.H.Y. Ong, J.A. Stampfli, P. Krummenacher, and B. Wellig, A Graphical Method for Combined Heat Pump and Indirect Heat Recovery Integration, *Energies (Basel)*. **15** (2022) 2829. doi:10.3390/en15082829.

[12] R. Agner, P. Gruber, and B. Wellig, Model Predictive Control of Heat Pumps with Thermal Energy Storages in Industrial Processes, *Energies (Basel)*. **17** (2024) 4823. doi:10.3390/en17194823.

[13] J.V.M. Walden, M. Bähr, A. Glade, J. Gollasch, A.P. Tran, and T. Lorenz, Nonlinear operational

optimization of an industrial power-to-heat system with a high temperature heat pump, a thermal energy storage and wind energy, *Appl Energy*. **344** (2023) 121247. doi:10.1016/j.apenergy.2023.121247.

[14] J.J. Aguilera, R. Padullés, W. Meesenburg, W.B. Markussen, B. Zühlsdorf, and B. Elmegaard, Operation optimization in large-scale heat pump systems: A scheduling framework integrating digital twin modelling, demand forecasting, and MILP, *Appl Energy*. **376** (2024) 124259. doi:10.1016/j.apenergy.2024.124259.

[15] R. Padullés, M.L. Hansen, M.P. Andersen, B. Zühlsdorf, J.K. Jensen, and B. Elmegaard, Optimal operation of industrial heat pumps with stratified thermal energy storage for emissions and cost reduction using day-ahead predictions, *Appl Therm Eng*. **266** (2025) 125703. doi:10.1016/j.applthermaleng.2025.125703.

[16] C. Schellenberg, J. Lohan, and L. Dimache, Operational optimisation of a heat pump system with sensible thermal energy storage using genetic algorithm, *Thermal Science*. **22** (2018) 2189–2202. doi:10.2298/TSCI171231272S.

[17] D. Olsen, P. Liem, Y. Abdelouadoud, and B. Wellig, Thermal Energy Storage Integration Based on Pinch Analysis - Methodology and Application, *Chemie Ingenieur Technik*. **89** (2017) 598–606. doi:10.1002/cite.201600103.

[18] T.G. Walmsley, M.R.W. Walmsley, M.J. Atkins, and J.R. Neale, Integration of industrial solar and gaseous waste heat into heat recovery loops using constant and variable temperature storage, *Energy*. **75** (2014) 53–67. doi:10.1016/j.energy.2014.01.103.

[19] B.S. Sadjjadi, J.-N. Gerdes, and A. Sauer, Energy flexible heat pumps in industrial energy systems: A review, *Energy Reports*. **9** (2023) 386–394. doi:10.1016/j.egyr.2022.12.110.

[20] L. Knorr, F. Schlosser, N. Horstmann, D. Divkovic, and H. Meschede, Flexible operation and integration of high-temperature heat pumps using large temperature glides, *Appl Energy*. **368** (2024) 123417. doi:10.1016/j.apenergy.2024.123417.

[21] W. Meesenburg, W.B. Markussen, T. Ommen, and B. Elmegaard, Optimizing control of two-stage ammonia heat pump for fast regulation of power uptake, *Appl Energy*. **271** (2020) 115126. doi:10.1016/j.apenergy.2020.115126.

[22] J.V.M. Walden, and P. Stathopoulos, The impact of heat pump load flexibility on its process integration and economics, *J Clean Prod*. **462** (2024) 142643. doi:10.1016/j.jclepro.2024.142643.

[23] J.V.M. Walden, B. Wellig, and P. Stathopoulos, Heat pump integration in non-continuous industrial processes by Dynamic Pinch Analysis Targeting, *Appl Energy*. **352** (2023) 121933. doi:10.1016/j.apenergy.2023.121933.

[24] P. Virtanen, R. Gommers, T.E. Oliphant, M. Haberland, T. Reddy, D. Cournapeau, E. Burovski, P. Peterson, W. Weckesser, J. Bright, S.J. van der Walt, M. Brett, J. Wilson, K.J. Millman, N. Mayorov, A.R.J. Nelson, E. Jones, R. Kern, E. Larson, C.J. Carey, Polat VanderPlas Jake, D. Laxalde, J. Perktold, R. Cimrman, I. Henriksen, E.A. Quintero, C.R. Harris, A.M. Archibald, A.H. Ribeiro, F. Pedregosa, P. van Mulbregt, and SciPy 1.0 Contributors, SciPy 1.0: Fundamental Algorithms for Scientific Computing in Python, *Nat Methods*. **17** (2020) 261–272. doi:10.1038/s41592-019-0686-2.

[25] M.L. Bynum, G.A. Hackebeil, W.E. Hart, C.D. Laird, B.L. Nicholson, J.D. Siirola, J.-P. Watson, and D.L. Woodruff, Pyomo–optimization modeling in python, Third, Springer Science & Business Media, 2021.

[26] W.E. Hart, J.-P. Watson, and D.L. Woodruff, Pyomo: modeling and solving mathematical programs in Python, *Math Program Comput*. **3** (2011) 219–260.

[27] Eurostat, Electricity prices for non-household consumers - bi-annual data (from 2007 onwards), (2025).

[28] Eurostat, Gas Prices for Non-Household Consumers - Bi-Annual Data (from 2007 onwards), (2025).

[29] Danish Energy Agency, Technology Data for Energy Storage, 2025. https://ens.dk/en/analyses-and-statistics/technology-data-energy-storage.

[30] P.H. Howard, and D. Sylvan, The economic climate: Establishing expert consensus on the economics of climate change, *Institute for Policy Integrity*. (2015) 438–441.

[31] IEA HPT Annex 58, High-Temperature Heat Pumps, (2023).

[32] VDI Heat Atlas, Springer Berlin Heidelberg, Berlin, Heidelberg, 2010. doi:10.1007/978-3-540-77877-6.

[33] M.P. Andersen, B. Zühlsdorf, W.B. Markussen, J.K. Jensen, and B. Elmegaard, Selection of working fluids and heat pump cycles at high temperatures: Creating a concise technology portfolio, *Appl Energy*. **376** (2024) 124312. doi:10.1016/j.apenergy.2024.124312.